

## **FINITE VOLUME METHOD FOR DETERMINING THE NATURAL CHARACTERISTICS OF STRUCTURES**

N. FALLAH

Civil Engineering Department, University of Guilan, P.O. Box 3756, Rasht, Iran  
E-mail: fallah@guilan.ac.ir

### **Abstract**

In this paper a finite volume based formulation is developed to calculate the structural natural characteristics including the natural frequencies and the critical buckling loads of slender beam/beam-columns in which the shear effects are taken into account. For natural frequency calculations, both shear effects and rotational inertia effects are considered. In this finite volume based approach, the equilibrium equations of control volumes are expressed and used with the boundary conditions to obtain the eigenvalue equation in the standard format. Then, the natural characteristics of beam/beam-columns are obtained by solving the eigenvalue equations. The formulation is tested on a number of benchmark problems. Accordingly, the proposed formulation has been found to accurately predict the natural frequencies and the critical buckling loads of the test problems. Also, the formulation is tested for the very thin and thick beams. It is found that the formulation is also able to analyze the thin beams in which no shear locks is observed.

Keywords: Finite volume, Natural frequency, Buckling load, Beam-column, Shear effect.

### **1. Introduction**

Natural frequency is one of the basic structural characteristics that affect the vibration behavior of a structure. This basic parameter dictates the body how to respond to the induced vibrations. Determining the natural frequencies, most importantly the lowest one, is not only important in civil engineering applications but also in applications of mechanical engineering, aerospace engineering, ship engineering and many industrial fields. In more general terms, this knowledge is necessary for any part of the body, even computer hard wares that may meet the environmental vibrations. In the field of structural dynamics, for finding the structural response due to a time dependant exciting force, there are methods in

which determining the values of structural natural frequencies is a prerequisite. Nowadays information about the natural frequencies of structures is even necessary for structural health monitoring purposes. This is due to the fact that once a defect starts in a component of the structural system; the system's natural frequencies are shifted. This phenomenon can be implemented for finding the damaged components and the damage intensity [1]. There are several methods for finding the system's natural frequencies that can be classified in three; including: analytical approaches, energy based approach and numerical methods. Each of these methods is divided into several sub-methods, where each one has its own capabilities and limitations depending to the application.

Recently, the calculation of structural natural frequency has received new attention by considering the uncertainties of the affecting factors which is a realistic view towards having a reliable knowledge about the system characteristics [2-4]. In these works for computing upper and lower bounds of the natural frequencies of a structure having material or geometric parameters which belong to the given intervals, the concept of interval mathematics is used. The given intervals of the properties lead the interval stiffness and mass matrices and the problem is transformed into a generalized interval eigenvalue problem. By solving the generalized interval eigenvalue problem, the bounds on the natural frequencies of the structure are calculated.

In addition to the structural natural frequencies, the critical buckling load is another characteristic that dictates the structural design. This characteristic is necessary to be studied both locally and globally in design of a structural system. Although, the subject of instability of structures has been investigated by researchers during the past decades, however, the subject is still under study by the researchers [5-11].

In this paper the finite volume (FV) method is extended to model the prismatic beam for the natural frequency calculations and also for the instability analysis of beam-columns. According to the works published previously on the application and the development of finite volume method (FVM) for structural problems, the method appears to have attractive features: the method is simple in terms of concept and formulation; and also it is shear locking free in the bending analysis of thin plates [12-14]. For the finite volume analysis, the beam/beam-column is meshed to a number of two-node line elements, which are regarded as control volumes or cells. Equilibrium equations of the cells are expressed explicitly and an approximate variation of section rotations and transverse displacements are assumed and introduced to the equilibrium equations. These approximated equations with boundary conditions are such arranged to yield a system of linear equations. The eigenvalue equation is then derived in the standard form that is solved to produce the natural frequencies and the buckling loads of the structure. The formulation is verified on a number of problems. This testing demonstrates the efficiency of the method in terms of accurate predictions and wide range of applicability.

## **2. Formulation**

### **2.1. Natural frequency calculation**

To establish a convenient equation that leads to finding the natural frequency of beam type structures numerically, the beam is discretized into a neighboring finite

volumes or cells, Fig. 1(a). A cell has connection to the nearest neighboring cells located on the right and left sides of the cell. The center of each cell is considered as computational point where the unknown variables are allocated to Fig. 1(b). At each computational point two degrees of freedom including transverse displacement  $w$  and section rotation  $\beta$ , are associated. The positive conventions for  $w$  and  $\beta$  are shown in Fig. 1(b).

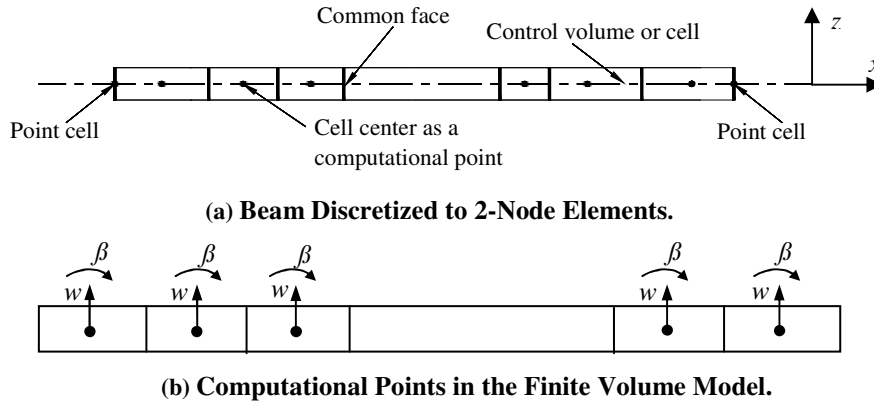


Fig. 1. Discretization of Beam.

In Fig. 2 an individual control volume is shown which is a part of a vibrating beam. The internal forces resulting from the stresses acting on faces which are common with the neighboring cells are also shown in Fig. 2. The dynamic equilibrium equation of this cell can be expressed as:

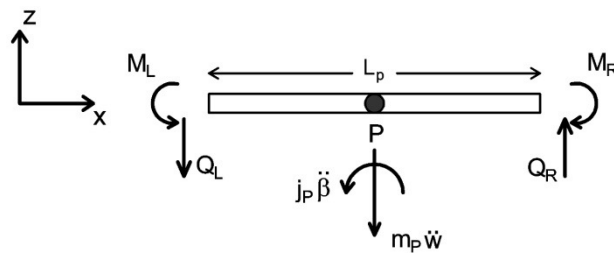


Fig. 2. An Individual Cell of the Beam with Acting Internal Forces.

$$\sum F_z = 0 \Rightarrow -m_p \ddot{w} - Q_L + Q_R = 0 \tag{1}$$

$$\sum M_y = 0 \Rightarrow -j_p \ddot{\beta} - M_L + M_R - (Q_L + Q_R)L_p / 2 = 0 \tag{2}$$

where  $m_p$  is the mass of cell and  $j_p$  is moment of inertia of the cell about the normal axis passing through the center of the cell. Also there are the following constitutive equations for a Timoshenko beam:

$$M_i = EI(d\beta/dx)_i \tag{3}$$

$$Q_i = Ak_s G(dw/dx + \beta)_i \tag{4}$$

in which  $EI$  is the flexural rigidity,  $G$  is the shear modulus,  $A$  is the cross sectional area and  $K_s$  is the shear correction factor which accounts for the nonuniform distribution of shear stress across the beam section. The shear correction factor is equal to 0.833 for solid rectangular cross section beam [15].

Prior to the substitution of Eqs. (3) and (4) into the equilibrium equations (1-2), it is necessary to apply a convenient procedure for the calculation of unknown values and their first order derivatives on the cell faces. In this regard, for a given face, a temporary 2-node isoparametric element is used where its nodes are located at the centers of two cells lying on either side of the face, Fig. 3. The temporary isoparametric element is referred to as interim element here.

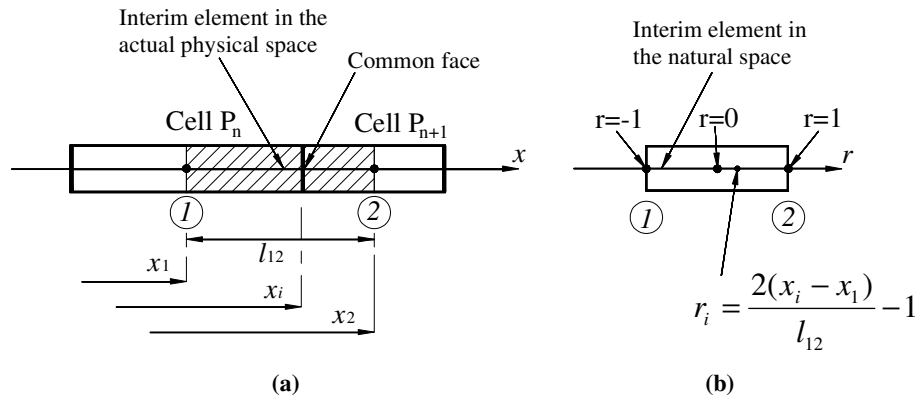


Fig. 3. Adjacent Cells and an Interim Element.

The idea of using interim element for the calculation of face values is quiet general which has been proposed by the author and used successfully in the cell centered finite volume formulation for plate bending analysis [14] and two dimensional loaded solids [16]. The interim element associated with the common face of the two neighboring cells,  $P_n$  and  $P_{n+1}$ , is shown in Fig. 3 The transverse displacement and section rotation are interpolated in the interim element as follows [15]

$$w = N_1 w_1 + N_2 w_2 = \sum_{i=1}^2 N_i w_i \tag{5}$$

$$\beta = N_1 \beta_1 + N_2 \beta_2 = \sum_{i=1}^2 N_i \beta_i \tag{6}$$

with

$$N_1 = \frac{1-r}{2} \quad ; \quad N_2 = \frac{1+r}{2} \tag{7}$$

where  $N_i$  is shape function and subscripts 1 and 2 denote the interim element node numbers in the natural space. The geometry of the interim element is also interpolated in the same way

$$x = N_1 x_1 + N_2 x_2 = \sum_{i=1}^2 N_i x_i \tag{8}$$

Using the chain rule of differentiation gives

$$\frac{d\beta}{dx} = \frac{d\beta}{dr} \frac{dr}{dx} = \left( \sum_{i=1}^2 \frac{dN_i}{dr} \beta_i \right) \frac{dr}{dx} \quad (9)$$

with

$$\frac{dx}{dr} = \sum_{i=1}^2 \frac{dN_i}{dr} x_i \quad (10)$$

Substituting Eq. (7) into Eq. (10) gives

$$\frac{dx}{dr} = \frac{x_2 - x_1}{2} = \frac{l_{12}}{2} \quad (11)$$

Then, using Eq. (11) in Eq. (9) results in

$$\frac{d\beta}{dx} = \frac{\beta_2 - \beta_1}{l_{12}} \quad (12)$$

In the same way, it can be shown that

$$\frac{dw}{dx} = \frac{w_2 - w_1}{l_{12}} \quad (13)$$

Therefore, for the right face of cell  $P$  in Fig. 3(a) which is not on the boundary, one can write:

$$\beta_R = (\beta_p + \beta_{p+1})/2 \quad (14)$$

$$(d\beta/dx)_R = (\beta_{p+1} - \beta_p)/(x_{p+1} - x_p) \quad (15)$$

$$(dw/dx)_R = (w_{p+1} - w_p)/(x_{p+1} - x_p) \quad (16)$$

### Boundary conditions

To introduce the boundary conditions to the solution procedure, point cells are used. The point cells are considered at the two ends of the beam, Figs. 1(a) and 4.

- For pinned end, we have:

$$w_{p_b} = 0 \quad (17)$$

$$M_{p_b} = 0 \quad (18)$$

where  $p_b$  indicates the point cell.

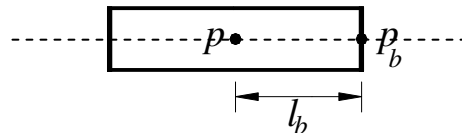


**Fig. 4. An Internal Cell Next to the Boundary and a Point Cell Considered at the Boundary.**

- For a clamped end we have:

$$w_{p_b} = 0 \quad (19)$$

$$\beta_{p_b} = 0 \quad (20)$$

- For a free end, we have:

$$M_{p_b} = 0 \quad (21)$$

$$Q_{p_b} = 0 \quad (22)$$

Substituting constitutive equations (3) and (4) into Eqs. (21) and (22) yields

$$\left( EI \frac{d\beta}{dx} \right)_{p_b} = 0 \quad (23)$$

$$\left[ K_s AG \left( \frac{dw}{dx} + \beta \right) \right]_{p_b} = 0 \quad (24)$$

Using approximating expressions of (12-13) in Eqs. (23) and (24) results in

$$\left[ EI n \left( \frac{\beta_{p_b} - \beta_p}{l_b} \right) \right]_{p_b} = 0 \quad (25)$$

$$\left[ K_s AG \left( \frac{n(w_{p_b} - w_p)}{l_b} - \beta_{p_b} \right) \right]_{p_b} = 0 \quad (26)$$

where  $n$  denotes unit outward normal to the boundary. When end-guided boundary condition is applied, two equations should be selected from the above equations, i.e., Eqs. (20) and (26).

By applying the boundary conditions for the two point cells, four equations are obtained. Equations associated with the internal cells and point cells provide a system of simultaneous linear equations, which relates the unknowns to one and other and can be expressed in the matrix form

$$\bar{\mathbf{M}}\ddot{\mathbf{u}} + \mathbf{R}\mathbf{u} = \mathbf{0} \quad (27)$$

in which vector  $\mathbf{u}$  includes the transverse displacements and section rotations of beam corresponding to center of cells. If we assume the vibration of beam in the following form:

$$\mathbf{u} = \bar{\mathbf{u}} \cos \omega t \quad (28)$$

Substituting Eq. (28) into Eq. (27) gives the following frequency equation:

$$\mathbf{R}\bar{\mathbf{u}} = \omega^2 \bar{\mathbf{M}}\bar{\mathbf{u}} \quad (29)$$

The above equation is a standard eigenvalue equation that can be solved for the natural frequency calculations using the standard computer programs.

## 2.2. Buckling load calculation

In this section we also use that model shown in Fig. 1 for the beam-column analysis. A generic cell in  $xz$  plane is shown in Fig. 5, which is under transverse uniform and concentrated loads  $q_p$  and  $F_k$ , respectively and also subjected to an axial load  $N$ . The stress resultant moments and forces acting on both sides of the cell are also shown where subscript  $R$  and  $L$  denote the right and left sides of the cell, respectively. The equilibrium equations of the cell can be represented by

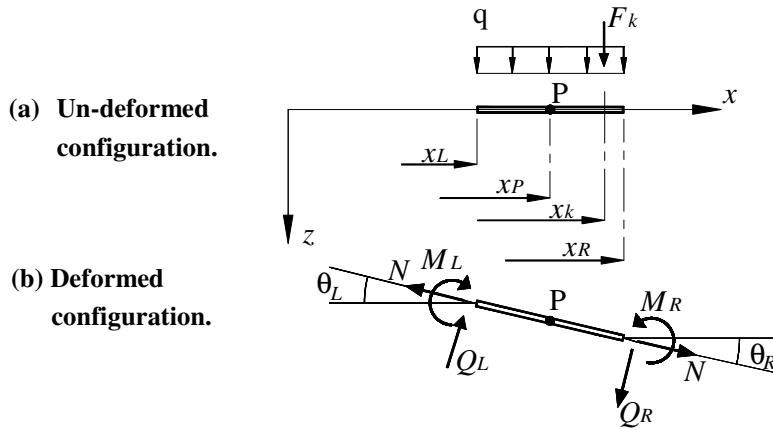


Fig. 5. Cell under External and Internal Loads.

$$\sum M_p = 0 \Rightarrow \sum_{i=L,R} [M_i n_i - Q_i n_i (x_i - x_p)] - \sum_{k=1}^{n.o.f} F_k (x_k - x_p) = 0 \quad (30)$$

$$\sum F_z = 0 \Rightarrow \sum_{i=L,R} [Q_i n_i \cos \theta_i + q n_i (x_i - x_p) + N n_i \sin \theta_i] + \sum_{k=1}^{n.o.f} F_k = 0 \quad (31)$$

where  $n_i$  indicates the unit outward normal to the left and right faces of the cell,  $n.o.f$  indicates the total number of the concentrated loads acting upon the cell. Due to the small deformation assumptions, we have

$$\cos \theta_i \approx 1, \quad \sin \theta_i \approx \left( \frac{dw}{dx} \right)_i \quad (32)$$

Substituting constitutive equations (3) and (4) into Eqs. (30) and (31), and using expressions (12-13) give two equations for each cell, which can be represented in the form of

$$\begin{bmatrix} R_{11} & R_{12} & \dots & R_{16} \\ R_{21} & R_{22} & \dots & R_{26} \end{bmatrix}_p \begin{bmatrix} \beta_{p-1} \\ w_{p-1} \\ \beta_p \\ w_p \\ \beta_{p+1} \\ w_{p+1} \end{bmatrix} = \begin{bmatrix} M \\ F \end{bmatrix}_p \quad (33)$$

or in the compact form

$$\mathbf{R}_p \mathbf{X}_p = \mathbf{B}_p \quad (34)$$

Equation (34) represents the relation of unknowns at the center of a cell to those at the centers of the two neighboring cells. It should be noted that the parameters  $M$  and  $F$  in Eq. (33) represents some constant values that may appear in Eqs. (30) and (31). An equation similar to Eq. (34) has been developed in [17] for the instability analysis of columns. This procedure is applied for all cells in the model, which provides two equations for each cell.

### 2.2.1. Boundary conditions

Implementation of boundary conditions for the instability analysis of beam-column is similar to the procedure explained for the frequency calculations. However, for the end with the known applied loads, the boundary conditions can be written more generally as:

$$M_{p_b} = M^* \quad (35)$$

$$Q_{p_b} = Q^* \quad (36)$$

where asterisked values denote the known applied values at the boundary. Substituting Eqs. (3) and (4) into Eqs. (35) and (36) yields

$$\left( EI \frac{d\beta}{dx} \right)_{p_b} = M^* \quad (37)$$

$$\left[ K_s AG \left( \frac{dw}{dx} + \beta \right) \right]_{p_b} = Q^* \quad (38)$$

By applying the approximated expressions of (12-13) in Eqs. (37) and (38) one can obtain:

$$\left[ EI n \left( \frac{\beta_{p_b} - \beta_p}{l_b} \right) \right]_{p_b} = M^* \quad (39)$$

$$\left[ K_s AG \left( \frac{n(w_{p_b} - w_p)}{l_b} - \beta_{p_b} \right) \right]_{p_b} = Q^* \quad (40)$$

where  $n$  denotes unit outward normal to the boundary. When mixed boundary conditions are applied, the same treatment as explained before is used.

Equations associated with the internal cells and point cells provides a system of simultaneous linear equations, which relates the unknowns to one and other and can be expressed in the matrix form

$$\mathbf{RX} = \mathbf{B} \quad (41)$$

where  $\mathbf{R}$  contains the coefficients relating the unknown variables associated with the cells. The vector  $\mathbf{X}$  contains the unknown variables and the vector  $\mathbf{B}$  represents the known values on the boundary and the values that dependant on the applied loads. The matrix  $\mathbf{R}$  has sparse nature and Eq. (41) can be solved by any appropriate solver technique for studying the bending behavior of the Timoshenko beam-columns. Moreover, this equation can be used for the calculation of buckling load of beam-columns, which is explained in the following section.

### 2.2.2. Calculation of buckling load

To calculate the buckling load, the matrix  $\mathbf{R}$ , the vectors  $\mathbf{X}$  and  $\mathbf{B}$  in Eq. (41) should be rearranged in the form of

$$\begin{bmatrix} \mathbf{R}_{11} & \mathbf{R}_{12} \\ \mathbf{R}_{21} & \mathbf{R}_{22} \end{bmatrix} \begin{bmatrix} \mathbf{w} \\ \boldsymbol{\beta} \end{bmatrix} = \begin{bmatrix} \mathbf{B}_1 \\ \mathbf{B}_2 \end{bmatrix} \quad (42)$$

where the vectors  $\mathbf{w}$  and  $\boldsymbol{\beta}$  contain the unknown variables, transverse displacement and section rotation, respectively.

The first equation from the matrix relation (42) is

$$\mathbf{R}_{11} \mathbf{w} + \mathbf{R}_{12} \boldsymbol{\beta} = \mathbf{B}_1 \quad (43)$$

Eliminating the sub-matrix  $\boldsymbol{\beta}$  from the above equation gives

$$\boldsymbol{\beta} = \mathbf{R}_{12}^{-1} [\mathbf{B}_1 - \mathbf{R}_{11} \mathbf{w}] \quad (44)$$

The sub-matrix  $\mathbf{R}_{11}$  can be resolved into two components

$$\mathbf{R}_{11} = \bar{\mathbf{R}} + N\tilde{\mathbf{R}} \quad (45)$$

Substituting Eq. (45) into Eq. (44) gives

$$\boldsymbol{\beta} = \mathbf{R}_{12}^{-1} [\mathbf{B}_1 - (\bar{\mathbf{R}} + N\tilde{\mathbf{R}}) \mathbf{w}] \quad (46)$$

Furthermore, substituting Eq. (46) into the second equation derived from Eq. (42) results in

$$\left[ (\mathbf{R}_{21} - \mathbf{R}_{22} \mathbf{R}_{12}^{-1} \bar{\mathbf{R}}) - N(\mathbf{R}_{22} \mathbf{R}_{12}^{-1} \tilde{\mathbf{R}}) \right] \mathbf{w} = \mathbf{B}_2 - \mathbf{R}_{22} \mathbf{R}_{12}^{-1} \mathbf{B}_1 \quad (47)$$

In the critical state it is expected that the determinant of Eq. (47) to vanish. By doing so, one can obtain the following equation:

$$\left[ (\mathbf{R}_{21} - \mathbf{R}_{22} \mathbf{R}_{12}^{-1} \bar{\mathbf{R}}) - N(\mathbf{R}_{22} \mathbf{R}_{12}^{-1} \tilde{\mathbf{R}}) \right] \mathbf{w} = \mathbf{0} \quad (48)$$

Eq. (48) can be represented in the following compact form:

$$\left[ \mathbf{A} - N\bar{\mathbf{A}} \right] \mathbf{w} = \mathbf{0} \quad (49)$$

which is a standard eigenvalue equation that can be used for the calculation of the buckling load using standard computer programs.

### 3. Numerical Examples

To verify the proposed formulation two test cases are studied by using a computer code developed based on the presented formulation. The results obtained are compared with the available analytical solutions in order to demonstrate the capability of the methods in the accurate predictions.

#### 3.1. Test case 1

In this test the natural frequencies of a pinned-pinned beam with rectangular cross section are calculated. The geometry and material properties of the beam are shown in Fig. 6.

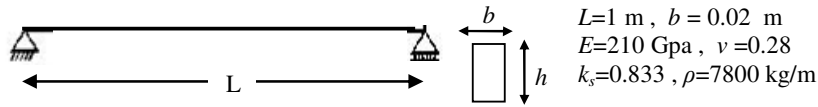


**Fig. 6. A pinned-pinned beam.**

The first three natural frequencies are obtained corresponding to  $h/l=0.001$  (thin beam) and  $h/l=0.1$  (thick beam). The results obtained are compared with the analytical values calculated using the following equation presented in [18]:

$$\Omega_n^4 \left(\frac{n\pi r}{l}\right)^4 \frac{E}{k_s G} - \Omega_n^2 \left[1 + \left(\frac{n\pi r}{l}\right)^2 \left(1 + \frac{E}{k_s G}\right)\right] + 1 = 0 \tag{50}$$

where  $\Omega_n = \omega'_n / \omega_n$ ,  $r$  is the radius of gyration of the beam cross section and  $n$  is the natural vibration mode number. The natural frequency of the beam is shown by  $\omega'_n$  in which the shear and rotational inertia effects are included and also by  $\omega_n$ , in which these effects are neglected.

The error of the predictions of the proposed approach is obtained as follows:

$$Error = \left(\frac{\omega_{fv}}{\omega'_n} - 1\right) \times 100 \tag{51}$$

where  $\omega_{fv}$  is the predicted frequency and  $\omega'_n$  is the frequency value calculated using Eq. (50). Different numbers of cells are used for the discretization of beam. The results obtained are shown in Fig. 7 for the thin beam and in Fig. 8 for the thick beam, respectively. As it can be seen the overestimated results converge monotonically to the analytical results as the number of cells is increased. It is noticeable that when a coarse mesh is applied the present method predicts the beam natural frequencies larger than the exact values, hence the upper bound property in the frequency predictions is observed.

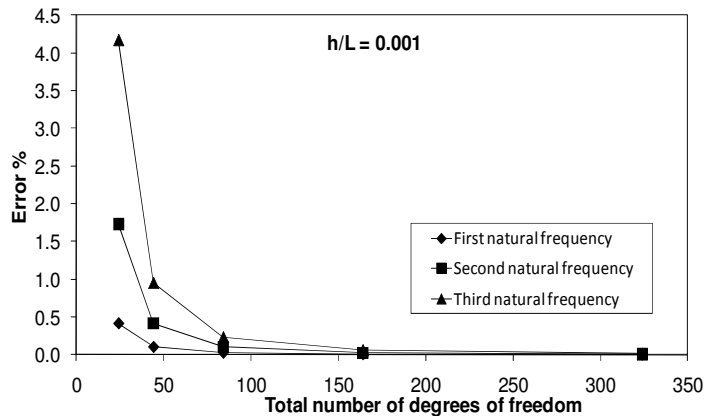


**Fig. 7. Convergence of the Present Predictions by Applying More Cells along the Thin Beam.**

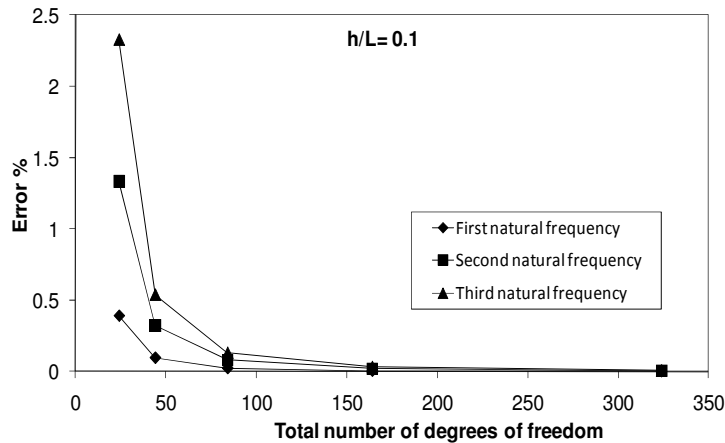


**Fig. 8. Convergence of the Present Predictions by Applying More Cells along the Thick Beam.**

### 3.2. Test case 2

This test concerns a pinned-pinned beam-column, which is subjected to a concentrated transverse load,  $F$ , at the mid-span and also loaded axially at the ends. The material properties and geometry of the beam are given in Fig. 9. The transverse load is considered constant and the mid-span transverse displacement,  $w$ , is computed corresponding to the different values of the axial load,  $N$ . The analytical relation of  $w-N$  is in the form of [19]:

$$w = \frac{F}{2NK} \left( \tan \frac{KL}{2} - \frac{KL}{2} \right) ; \quad K = \sqrt{\frac{N}{EI}} \quad (52)$$

in which the shear effects are excluded. It should be mentioned that in this test it is assumed that the buckling of the beam-columns is constrained about the sectional minor axis and also there is no yielding occurrence. The beam-column is analyzed using the procedure presented and the vertical displacement of the mid-span is obtained and compared with the values given by Eq. (52) corresponding to the assumed constant transverse loads. To exclude the shear effects in the results of present formulation, a very large value of shear modulus is assumed. As can be seen in Fig. 9, the results obtained are in close agreement with the analytical values. Also Fig. 9 shows the nonlinear relation of the transverse deflection and the axial load due to the dependence of the bending moment on the transverse displacement. It is seen that the curves converge to the analytical buckling load value, 1644.93 kN. It is also observed that applying different transverse load values do not affect the limit that those curves are converging to, as expected.

The buckling load of the beam-column is also evaluated using the eigenvalue equation (49). The buckling loads with and without shear effects are computed using different meshes of equal elements. The errors in the overestimated predictions are computed in comparison with the analytical

values taken from Timoshenko [19]. Figure 10 illustrates how the error diminishes as the number of degrees of freedom is increased by mesh refinement. It should be noted; Fig. 10 demonstrates the present formulation is able to predict, nearly with the same accuracy, the column buckling capacity whether the shear effects are considered or not. This dual capability of the present method is obtained by adjusting the shear modulus value as it has been already used for the results presented in Fig. 9. It should be mentioned that when a coarse mesh is applied the present formulation predicts the column buckling loads larger than the exact values; hence the upper bound property in the buckling load predictions is observed similar as in the previous test.

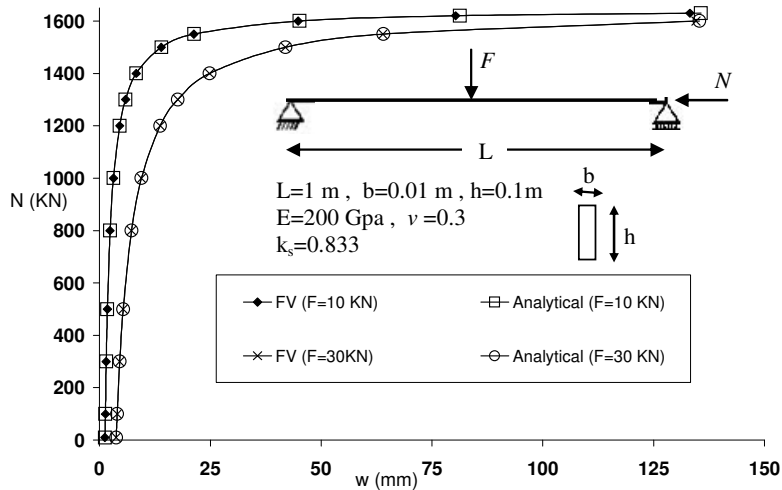


Fig. 9. Load-Deflection Curve for a Pinned-Pinned Beam-Column.

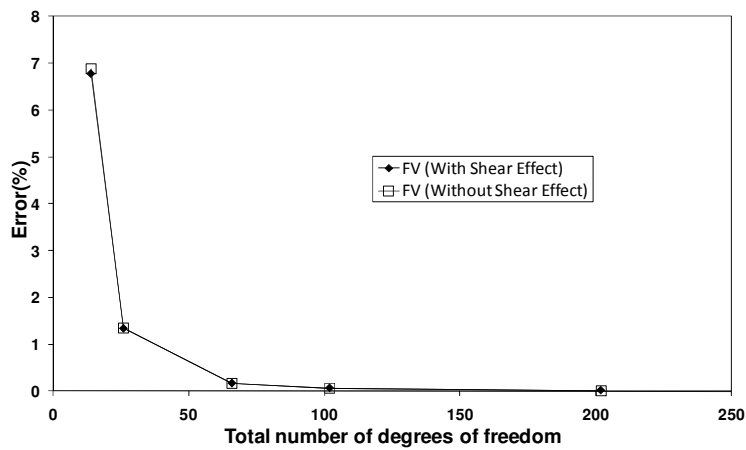


Fig. 10. Error in the Prediction of Buckling Load of a Pinned-Pinned Column with and without Shear Effects.

#### 4. Conclusions

A finite volume based formulation has been developed for the calculation of structural natural characteristics including natural frequencies for beam type structures and buckling loads for beam-columns. Timoshenko beam theory has been applied in which both rotational inertia and shear effects are considered in natural frequency calculations and also shear effects are considered for the buckling analysis. The analysis of the test problems has shown that:

- The proposed formulations are able to provide comparable predictions for both natural frequencies and buckling loads.
- It has been observed that by applying finer meshes, the predictions converge to the analytical predictions monotonically.
- The results obtained reveal that the finite volume method can successfully predict both natural characteristics with upper bound properties.

#### References

1. Doebling, S.W.; Farrar, C.R.; Prime, M.B.; and Shevitz, D.W. (1996). Damage identification and health monitoring of structural and mechanical systems from changes in their vibration characteristics: A literature review. *Report no. LA-13070-MS*, Los Alamos National Laboratory.
2. Qiu, Z.P.; Chen, S.H.; and Elishakoff, I. (1995). Natural frequencies of structures with uncertain but nonrandom parameters. *Journal of Optimization Theory and Applications*, 86(3), 669-683.
3. Qiu, Z.P.; Wang, X.; and Friswell, M.I. (2005). Eigenvalue bounds of structures with uncertain-but-bounded parameters. *Journal of Sound and Vibration*, 282(1-2), 297-312.
4. Gao, W. (2007). Natural frequency and mode shape analysis of structures with uncertainty. *Mechanical Systems and Signal Processing*, 21(1), 24-39.
5. Bažant, Z.P. (2000). Structural stability. *International Journal of Solids and Structures*, 37(1-2), 55-67.
6. Thompson, S.P.; and Loughlan, J. (1995). The active buckling control of some composite column strips using piezoceramic actuators. *Composite Structures*, 32(1-4), 59-67.
7. Maretic, R.B.; and Atanackovic, T.M. (2001). Buckling of column with base attached to elastic half-space. *Journal of Engineering Mechanics*, 127(3), 242-247.
8. Wang, Q. (2002). On buckling of column structures with a pair of piezoelectric layers. *Engineering Structures*, 24(2), 199-205.
9. Wang, Q.; and Quek, S.T. (2002). Enhancing flutter and buckling capacity of column by piezoelectric layers. *International Journal of Solids and Structures*, 39(16), 4167-4180.
10. Al-Sadder, S.Z. (2004). Exact expressions for stability functions of a general non-prismatic beam-column member. *Journal of Constructional Steel Research*, 60(11), 1561-1584.

11. Przybylski, J. (2008). Stability of an articulated column with two collocated piezoelectric actuators. *Engineering Structures*, 30(12), 3739-3750.
12. Wheel, M.A. (1997). A finite volume method for analysing the bending deformation of thick and thin plates. *Computer Methods in Applied Mechanics and Engineering*, 147(1-2), 199-208.
13. Fallah, N. (2004). Cell vertex and Cell centred finite volume methods for plate bending analysis. *Computer Methods in Applied Mechanics and Engineering*, 193(33-35), 3457-3470.
14. Fallah, N. (2006). On the use of shape functions in cell centered finite volume formulation for plate bending analysis based on the Mindlin-Reissner plate theory. *Computers & Structures*, 84(26-27), 1664-1672.
15. Bathe, K.J. (1996). *Finite element procedures*. Prentice-Hall, New Jersey.
16. Fallah, N. (2008). A method for the calculation of face gradients in the two dimensional cell centred finite volume formulation for the stress analysis in solid problems. *Scientia Iranica: International Journal of Science and Technology*, 15(3), 286-294.
17. Fallah, N.; and Hatami, F. (2006). Extension of the finite volume method for instability analysis of columns with shear effects. *Proceedings of the 8<sup>th</sup> International Conference on Computational Structures Technology, Paper 192*, Spain.
18. Chopra, A.K. (2001). *Dynamics of Structures: Theory and applications to earthquake engineering*. (2<sup>nd</sup> Ed.), Prentice Hall.
19. Timoshenko, S.P.; and Gere, J.M. (1961). *Theory of elastic stability*. (2<sup>nd</sup> Ed.), McGraw-Hill.